Damghan University Press

Journal of Nano Simulation
journal homepage: jons.du.ac.ir

Volume 2, Issue 1, Winter 2026, 1-14
DOI: 10.22128/jons.2025.1010.1008

# Engineering the electronic nanostructure band gap dependence of doped graphene. A DFT investigation by pseudopotentials GGA results

Babak Minaie[1,*], Reza Kalami[1] and José M. De Sousa [2]
[1]*School of Physics, Damghan University, Damghan, Iran*

[2]*Instituto Federal de Educação, Ciência e Tecnologia do Piauí – IFPI, Primavera, São Raimundo Nonato, 64770-000, Piauí, Brazil*

## HIGHLIGHTS

- Density functional theory is used to study electronic band structure engineering in doped graphene
- Element-specific substitutional doping effectively modifies graphene electronic properties
- Selected dopants induce band-gap opening and transitions to semiconducting behavior
- Rare-earth and light-element dopants show strong contributions near the Fermi level
- The results provide guidance for graphene-based nanoelectronic material design

## GRAPHICAL ABSTRACT

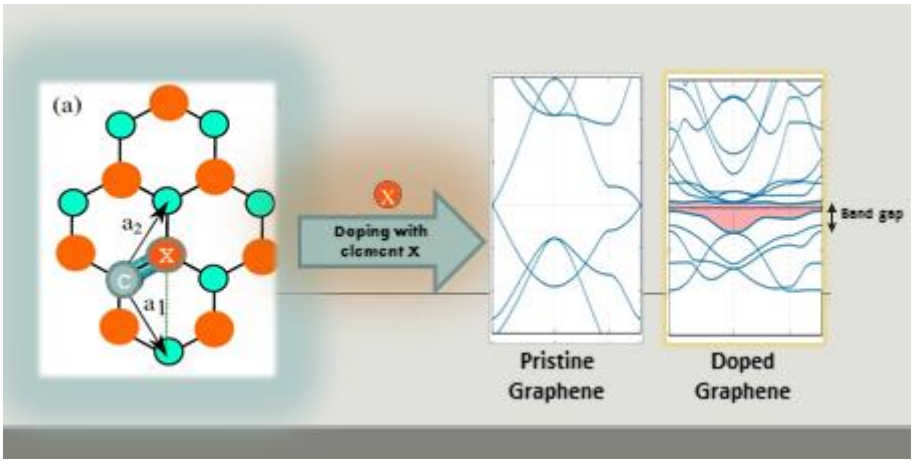


## ARTICLE INFO

*Article history:*
Received: 2025-05-10
Received in revised form: 2025-10-12
Accepted: 2025-12-19

Available online: 2026-01-01

*Keywords:*
*Vibration analysis,*
*Single-layer nanoribbon,*
*Molecular dynamics simulation,*
*Two-phase elasticity theory,*
*local mixture parameter.*

## ABSTRACT

In this study, we systematically investigate the effects of doping single-layer graphene with a broad range of chemical elements on its electronic band structure using density functional theory (DFT) within the generalized gradient approximation (GGA) pseudopotential framework. We substitute carbon atoms in the graphene lattice with 55 different elements spanning alkali metals, alkaline earth metals, transition metals, rare earth elements, semimetals, nonmetals, halogens, and noble gases. Due to the diversity of effects observed, the analysis focuses on selected representative dopants that exhibit distinct modifications of electronic properties and band gap behavior. Our results show that while pristine graphene is gapless and exhibits semi-metallic behavior, doping with specific elements—such as hydrogen and certain transition metals—can induce significant changes including band gap opening and transitions to conductive or semiconducting states. These findings highlight the powerful tunability of graphene's electronic properties via element-specific doping, offering promising routes for engineering graphene-based materials in next-generation nanoelectronic devices.

* *babminaie@std.du.ac.ir*

## 1. Introduction

The groundbreaking discovery of a single layer of graphite, known as graphene, synthesized by Novoselov, K. S., Geim, A. K., et al. in 2004 and their collaborators, has opened up a new frontier in nanoelectronic engineering and the development of novel nanostructures and materials [1]. Both theoretical and experimental studies have demonstrated graphene's exceptional electronic properties, placing it as one of the most promising materials for the advancement of nanoelectronics and various applications due to its unique characteristics [2]. Properties such as the anomalous quantum Hall effect [3], well-defined optical absorption [4], and Klein tunneling [5] are among the key features that contribute to graphene's superb electrical and thermal conductivity as well as its excellent gas barrier properties [6]. As a result, graphene holds significant potential for the sustained progress and diversification of materials in the field of nanoelectronics.

Graphene show extremely high charge carrier mobility ($2 \times 10^5 \mathrm{cm^2 V^{-1} s^{-1}}$) [7], low $\frac{1}{f}$ ($f$ is frequency) noise [8] and high saturation velocity, their nanostructure-based material are attractive for several applications in electronic circuits and communication [9]. Furthermore, graphene is one nanostructure-based and/or material that possesses great mechanical proper- ties. Lee, C., Wei, X., Kysar, J. W., and Hone, J. (2008), measured the elastic properties of graphene single-layer by nanoindentation in an atomic force microscope, approximately 1.0 TPa [10]. Lee, J. U., Yoon, D., and Cheong, H. (2012), investigated the Young's modulus of graphene is estimated by measuring the strain applied by a pressure difference across graphene membranes using Raman spectroscopy. Estimated Young's modulus values of single and bi-layer graphene are $2.4 \pm 0.4$ TPa and $2.0 \pm 0.5$ TPa, respectively [11]. Jiang, J. W., Wang, J. S., and Li, B. (2009), investigate the Young's modulus of graphene single-layer from intrinsic thermal vibration in honeycomb lattice performed by molecular dynamics method, 0.95 to 1.1 TPa [12]. De Sousa, J. M. (2021), using fully reactive (ReaxFF) Classical Molecular Dynamics Simulations Method, obtained around 1.095 TPa at room temperature [13]. The graphene single layer has good thermal conductivity properties. Balandin, A. A., Ghosh, S., Bao, W., Calizo, I., Teweldebrhan, D., Miao, F., and Lau, C. N. (2008), obtained thermal properties about $((4.84 \pm 0.44)\times10^3$ to $(5.30\pm0.48)^3$ W/mK) [14]. Wang, X., Zhi, L., and Mullen, K. (2008), showed that experimental techniques, that the single-layer graphene is widely used in practical applications according to its chemical properties, such as its high surface and volume ratio [15]. Craciun, M. F., Russo, S., Yamamoto, M., and Tarucha, S. (2011), present in their work that the electronic properties serving for next generation nanoelectronic devices [16]. Zhan, D., Yan, J., Lai, L., Ni, Z., Liu, L., and Shen, Z. (2012), show that despite the band gap null in graphene single layer, new theoretical and experimental investigations with the objectives of controllable tuning of electronic properties of graphene single-layer based on modifying its electronic nanostructure become highly important [17].

Nevertheless, the controllable tuning of electronic properties of graphene based on modifying its electronic structure becomes highly important. Currently, research carried out focuses as main objectives on methods that make it possible to modify the electronic properties of graphene, such as, applying electric and magnetic fields, tuning the electronic structure and carrier concentration by chemical intercalation, controlling the stacking geometry of bilayer graphene, adjusting the concentration and types (vacancy, covalent bonds) of defects, applying strain [17]. Wang, X., Sun, G., Routh, P., Kim, D. H., Huang, W., and Chen, P. (2014), show that the heteroatom doping can endow graphene with various new or improved electromagnetic, physicochemical, optical, and structural properties [18]. Putri, L. K., Ong,W. J., Chang, W. S., and Chai, S. P. (2015), show that doping graphene with foreign atoms extends its function in the photocatalyst system [19]. Shao, Y., Zhang, S., *et. al* (2010), showed that nitrogen-doped graphene is an excellent electrochemical performance [20]. Kumar, R., *et. al* (2020), showed that heteroatom-doped graphene play a substantial role in several science fields [21]. In a comparative context, Vargas-Bernal et al. (2015/2016) reviewed the electronic and structural properties of graphene relative to other two-dimensional materials (silicene, germanene, phosphorene, h-BN, TMDs etc.), highlighting that while many 2D semiconductors inherently possess finite band gaps, graphene requires engineering (e.g. doping, strain) to open a gap [22]. Similarly, in the study by Wang et al. (2019), doping graphene with B, Al, Si, Ge, As, and Sb and applying external electric fields yielded band gaps ranging from ~0.68 eV to ~1.58 eV, with tunability under fields (e.g. Sb-G reaching ~1.84 eV under 1.2 eV/Å) [23].

The novelty of the present work lies in its protocol-consistent screening approach: using the same DFT-GGA pseudopotential methodology we survey a broad set of chemical elements to identify representative dopants that induce distinct modifications in the electronic band structure of single-layer graphene. While this manuscript reports detailed results for selected representative cases, the comparative framework enables extraction of general trends across dopant classes (metals, nonmetals, semimetals, halogens), offering a

practical map for subsequent, targeted theoretical and experimental studies in graphene band-gap engineering.

Herein this research article, we seek to contribute to our results, aiming to investigate the nanostructural stability and electronic band nanostructure engineering of doped graphene single-layer, analyzing its electronic structure for interactions between the carbon atom and

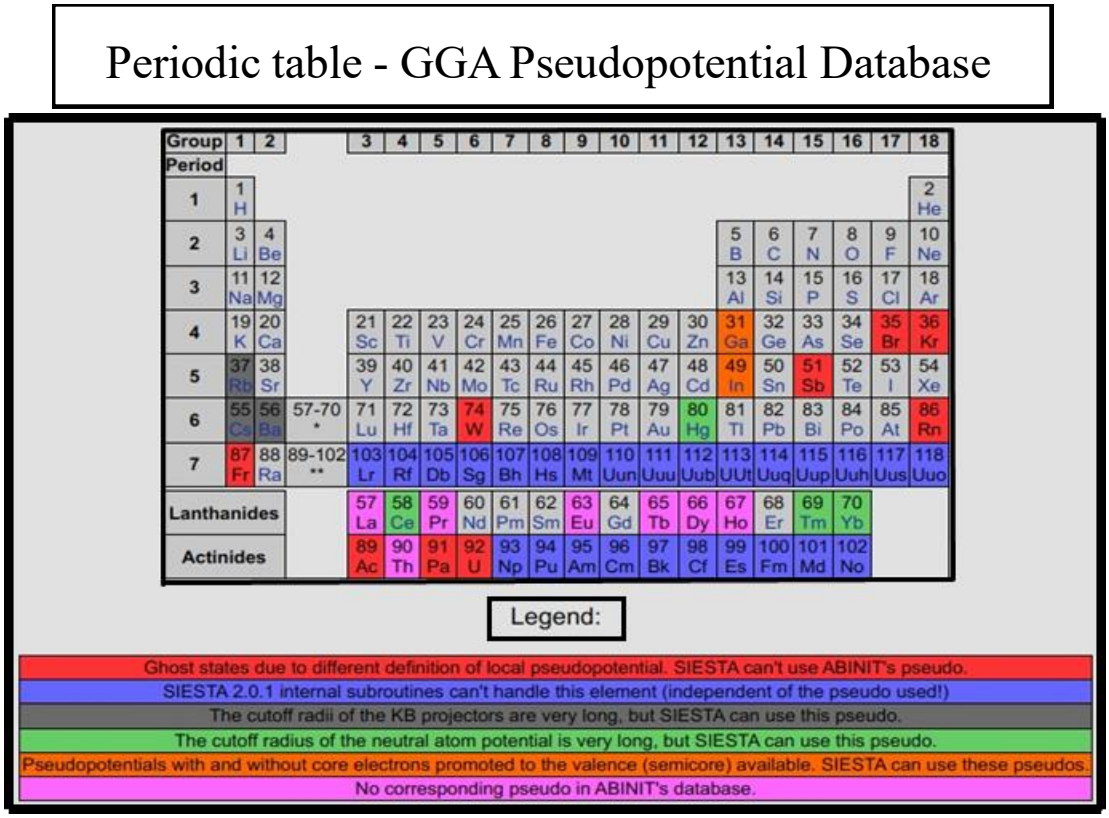


**Figure 1**: adapted from the page that contains links to pseudopotentials which were obtained from Abinit's pseudo database. (GGA Pseudopotential Database)

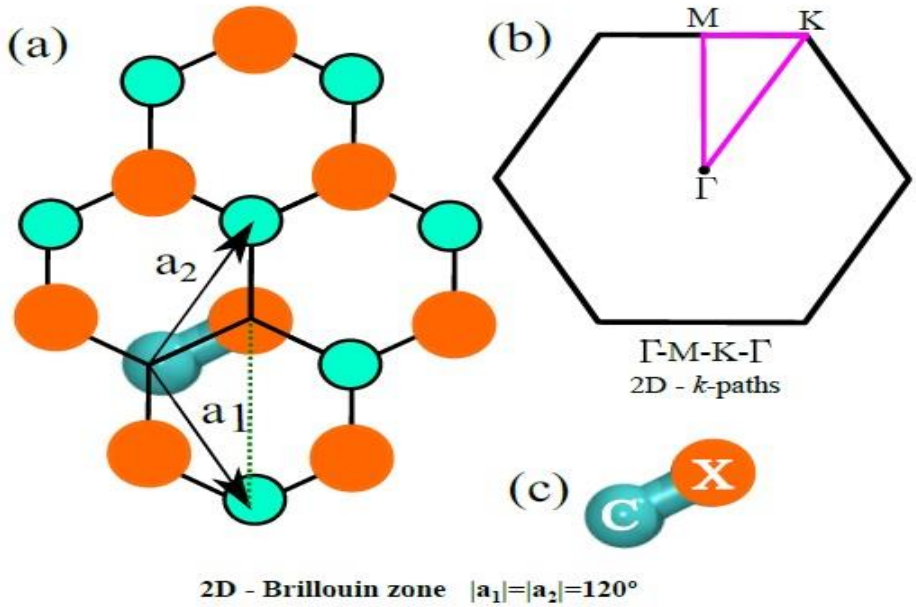


**Figure 2**: Schematic illustration of doping in the graphene single-layer. The cyan color represents carbon atom and the orange circle (X-atom) is substitution heteroatom doped graphene single-layer (in unit cell).

an arbitrary atom X-type doping from the periodic table (see Figure 1 and Figure 2).

## 2. Model and the computational details

To determine the nanostructural stability and electronic band nanostructure engineering of doped graphene single-layer, was carried out a systematic study using a DFT framework [24, 25] as implemented in the SIESTA code [26, 27, 28]. While DFT is a reliable and extensively used tool for studying the electronic structure of materials, it is known to have limitations, especially in predicting excited-state properties and in systems with strong electron correlations. Therefore, our results provide initial theoretical insights, and we recommend further studies using advanced methods such as GW or hybrid functionals, as well as experimental validation to confirm the findings. It should be noted that while the GGA-PBE pseudopotential approach provides a reasonable description of the structural and energetic properties of doped graphene, it generally underestimates the band gap values due to the approximate treatment of exchange–correlation effects. In addition, the pseudopotential approximation may not completely account for semi-core states in some dopant atoms, slightly influencing the calculated electronic levels. These well-recognized limitations suggest that more sophisticated approaches, such as hybrid functionals or GW corrections, could further refine the results [29].

We performed extensive computational calculations on doping graphene with 55 elements using the GGA pseudopotential database (see Figure 1). These elements represent a broad range of chemical groups: alkali metals, alkaline earth metals, transition metals, rare earth elements, and main group elements including semimetals, nonmetals, halogens, and noble gases. The doping involved substituting carbon atoms in the graphene unit cell with these elements to systematically investigate the resulting electronic band structure modifications. In the main text, we focus on representative dopants that demonstrate distinct and significant effects on the band gap and electronic properties, selecting them based on the diversity of their electronic contributions and band gap modulation behavior. The Kohn-Sham orbitals were expanded in a double-ζ basis set composed of numerical pseudoatomic orbitals of finite range enhanced with polarization orbitals. A common atomic confinement energy shift of 0.02 Ry was used to define the basis function cutoff radii, while the fineness of the real space grid was determined by a mesh cutoff of 400 Ry [30]. For the exchange-correlation potential, we used the generalized gradient approximation [31] and the pseudopotentials were modeled within the norm-conserving Troullier-Martins [32] scheme in the Kleinman-Bylander factorized form [33]. Brillouin-zone integrations were performed using a Monkhorst-Pack grid of 1 × 1 × 36 k-points [34]. Doping in the graphene single-layer follows the scheme illustrated in Figure 2. Where the orange circles will be replaced by (X) atoms (GGA Pseudopotential Database).

Graphene is a layer of carbon (extracted from graphite) that consists of a honeycomb nanostructure lattice with the nearest carbon-to-carbon distance of 1.42Å(see Figure 3). The unit cell of graphene contains 2 equivalent carbon atoms (see in Figure 3). This crystal nanostructure of the unit cell of graphene (bipartite lattice), results in the touching between bonding ($\pi$) and anti-bonding ($\pi^*$) orbitals at each energy valleys K and $K_j$ when considering hopping only occurs between the nearest neighbor atomic sites [1]. The $\pi$ bands of 2D graphene single layer are derived from the following 2×2 Hamiltonian matrix [35, 36]. The $\pi$ electrons of low-energy bands around K and $K_j$ can be described mathematically by the Dirac-like Hamiltonian [1]:

$$\mathcal{H}_{\kappa} = \hbar v_f \begin{pmatrix} 0 & K_x - iK_y \\ K_x + iK_y & 0 \end{pmatrix} \quad (1)$$

$$\mathcal{H}_{\kappa'} = -\hbar v_f \begin{pmatrix} 0 & K_x + iK_y \\ K_x - iK_y & 0 \end{pmatrix} \quad (2)$$

where, the K is the nearest-neighbor interaction between the sites (carbon 1 and carbon 2 atoms in the unit cell) sublattices is expressed mathematically as:

$$K = \gamma_0 \left[ e^{ik_x a/\sqrt{3}} + 2e^{-ik_x a/2\sqrt{3}} cos\left(\frac{k_y a}{2}\right) \right] \quad (3)$$

where a = $(1.42 \times \sqrt{3})$Å, is the lattice constant and $\gamma_0$ is nearest-neighbor transfer integral energy dispersion relation of graphene single layer, $E_{2D}(k_x, k_y)$:

$$E_{2D}(k_x, k_y) = \pm\gamma_0 \sqrt{1 + 4cos\left(\frac{\sqrt{3}k_x a}{2}\right) cos\left(\frac{k_y a}{2}\right) + 4cos^2\left(\frac{4k_y a}{2}\right)} \quad (4)$$

so, we fold the Brillouin zone of graphene single layer and introduce discrete values of the wave vector in the direction perpendicular to the nanostructure hexagonal axis (see Figure 3). We obtained as a result, a set of 1D energy dispersion relations is obtained by slicing up the 2D energy band structure of graphene single layer in the circumferential direction. In Figure 3 (a) we showed the real space unit cells and Brillouin zones for zig-zag graphene, where the $|\vec{a}_1|$ and $|\vec{a}_2|$ , are unit vectors and/or reciprocal vectors of the original graphene single layer. Writing the following relation for the periodic boundary condition associated with the armchair and zigzag graphene single layer, are follow, respectively:

$$k_x^m = \frac{m}{N_x}\frac{2\pi}{\sqrt{3}a}, \quad (m = 1, \dots\dots, N_x) \tag{5}$$

$$k_x^m = \frac{m}{N_y}\frac{2\pi}{2a}, \quad (m = 1, \dots\dots, N_y) \tag{6}$$

The energy bands for the armchair and zigzag $E_m^A(k)$ and $E_m^Z(k)$ can be obtained mathematically, respectively follow:

$$E_m^A(k) = \pm\gamma_0\sqrt{1 \pm 4cos\left(\frac{m\pi}{5}\right)cos\left(\frac{ka}{2}\right) + 4cos^2\left(\frac{4ka}{2}\right)}, \quad (-\pi < ka < \pi)\ (m = 1, \dots.,5) \tag{7}$$

$$E_m^Z(k) = \pm\gamma_0\sqrt{1 \pm 4cos\left(\frac{\sqrt{3}ka}{5}\right)cos\left(\frac{m\pi}{9}\right) + 4cos^2\left(\frac{m\pi}{9}\right)}, \quad \left(-\frac{\pi}{\sqrt{3}} < ka < \frac{\pi}{\sqrt{3}}\right)\ (m = 1, \dots.,9) \tag{8}$$

The sign "positive" and "negative" for both are like Hamiltonian resembles the spinor functions in quantum electrodynamics, and it can be considered as an extra degree of freedom which is pseudospins [37]. Thus, we obtain the results as linearly dispersive electronic band structure at low-energy regime around K and K' (see Figure 3). The energy can be expressed by $E = \pm vFK$, which indicates the low-energy carriers in graphene is zero-mass and its speed is independent of energy. The gapless graphene displays ambipolar electric field effect with property extremely high mobility at 300 K as observed experimentally [38]. Based on the theoretical foundation presented for graphene's electronic band structure, it is possible to dope the graphene single layer by electrons or holes with tunable charge concentration, and the maximum can exceed $10^{13}$ cm$^2$ [39]. Therefore, the electronic band structure of these parabolic bands (see Figure 3) can be modified by tuning the electronic coupling between X-type atom doped by the elements from the available Periodic Table bonded with carbon atom breaking the unit-cell symmetry chemically, can intentionally modify the corresponding electronic band structure of graphene (see Figure 2). So, single layer graphene is a naturally two-dimensional system formed by carbon atoms periodically organized in a hexagonal network, where calculations carried out using the DFT method show a band structure composed of Dirac cones that touch each other at the extremes of the Brillouin zone. Thus, in Figure 3, we present the electronic band structure for pristine graphene. In Figure 3, panel (a) shows the two-dimensional Brillouin zone, (b) illustrates the k-paths used in the band structure calculation,

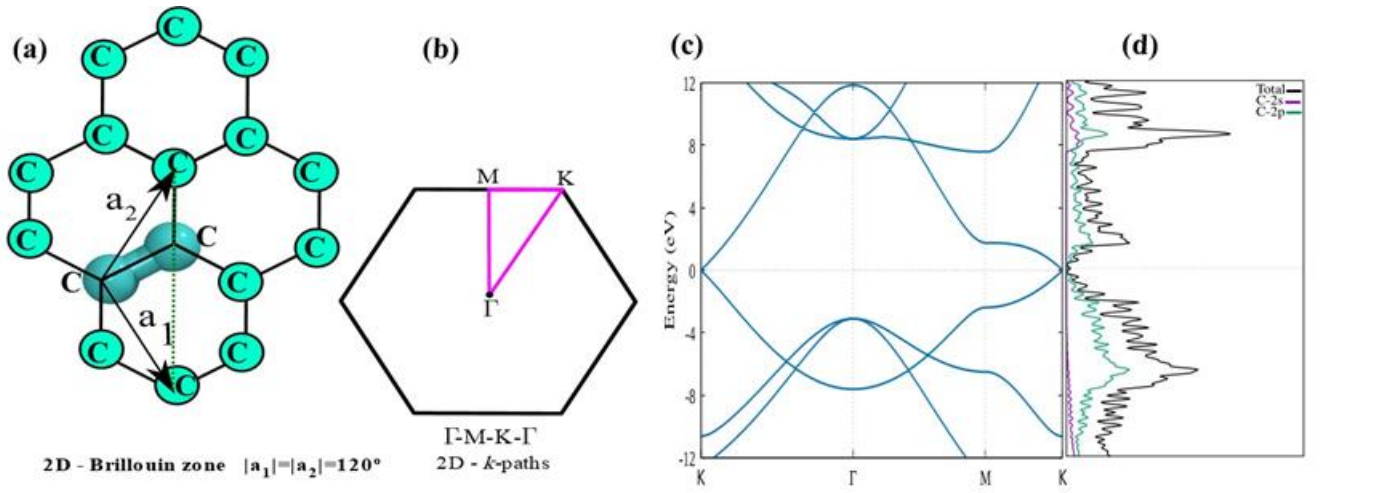


**Figure 3***:* The electronic band structures of graphene single-layer. (a) Schematic illustration showed the reciprocal lattice vectors and the corners of the first Brillouin zone. (b) 2D-k-paths representation. (c) Electronic band structure. (d) partial density of states (PDOS) of C orbitals

and (c) presents the corresponding electronic band structure of graphene. Graphene, a single layer of carbon atoms arranged in a densely packed hexagonal lattice, exhibits a unique semi-metallic nature arising from the intersection of the π and π* bands at the Fermi level at the K and K′ points in the reciprocal space. The linear dispersion of the bands near these points leads to zero effective mass quasiparticles (Dirac fermions), which result from the equivalence of the two sublattices in the primitive unit cell of graphene. The spacing and curvature of the energy bands play a crucial role in determining

the material's electronic behavior. The absence of a band gap at the Dirac point confirms its semi-metallic character, while the nearly linear shape of the bands near the Fermi energy reflects the high mobility of charge carriers. Furthermore, the overall symmetry of the band structure mirrors the hexagonal symmetry of the graphene lattice. Figure 3(d) shows the total and partial density of states (PDOS) of graphene. The black curve represents the total DOS, while the purple and teal curves correspond to the C-2s and C-2p orbital contributions, respectively. The strong peaks near the Fermi level originate mainly from the C-2p states, indicating that π bonding dominates the electronic structure. The 2s orbitals contribute primarily to deeper energy levels (below –10 eV). The relative intensity of the 2p contribution suggests strong covalent bonding, which is typical in 2D carbon materials and underpins graphene's remarkable electrical

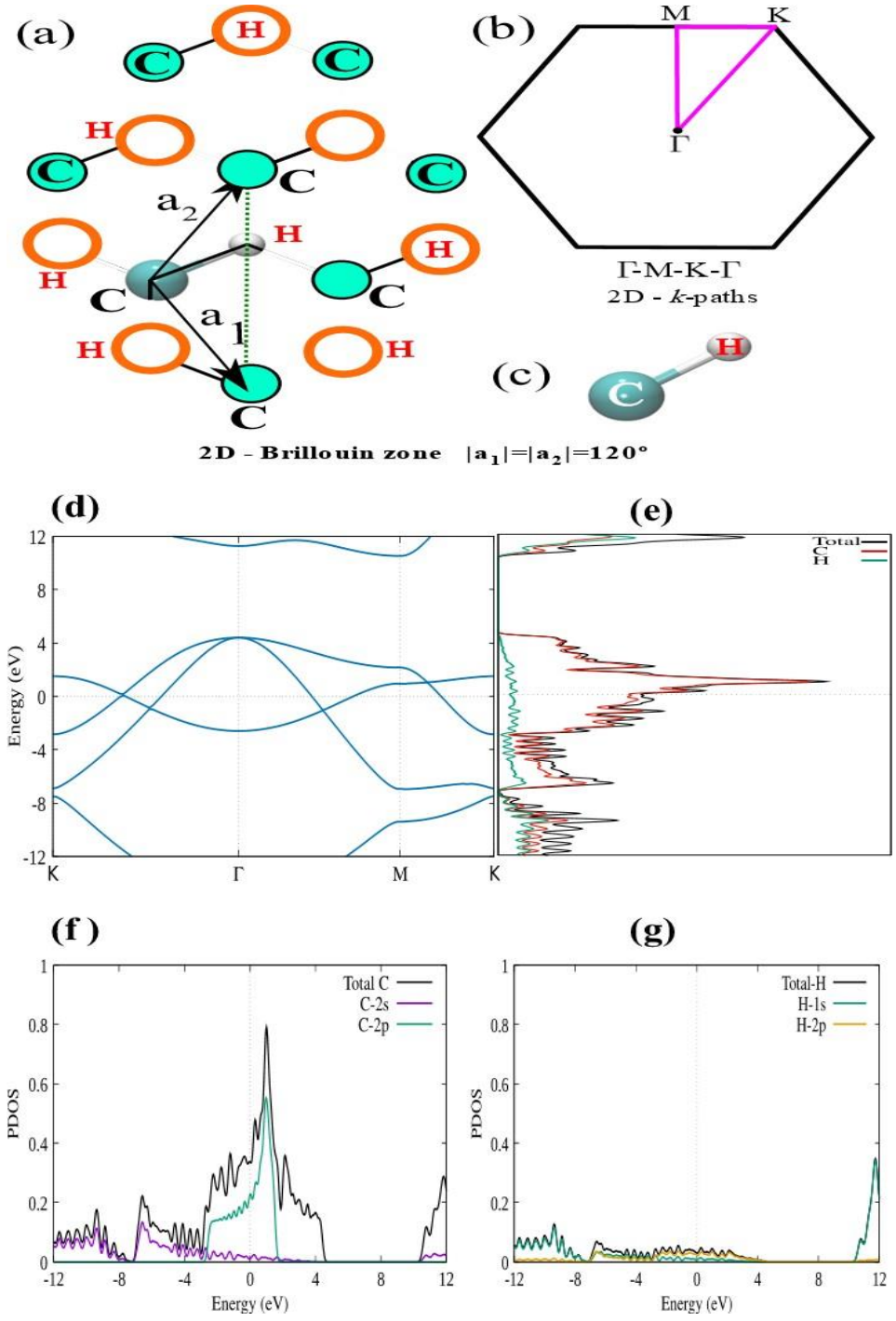


**Figure 4:** The electronic band structures of graphene single-layer doped C-H. (a) Schematic illustration showed the reciprocal lattice vectors and the corners of the first Brillouin zone. (b) 2D-k-paths representation. (c) CPK fully atomistic visualization of C-H bonded. (d) Electronic band structure and (e) density of states (DOS) and partial DOS (PDOS) of graphene single layer doping by H atom. PDOS of (f) C atom and (g) H atom in graphene single-layer doped C−H

conductivity and mechanical strength. Graphene has similarities with photons in connection with linear energy-momentum scattering the relativistic Dirac condition describes free space. The superior electrical structure of graphene, have had a significant impact on the new integer quantum Hall impact [40].

The electronic characteristics of single layer graphene doped (by chemical elements: alkali metals, alkaline earth metals, transition metals, Rare-earth elements and semimetals, nonmetals, halogens, noble gases and unknown chemical properties elements) were studied using the DFT method. Thus, according to Figure 2, we doped the

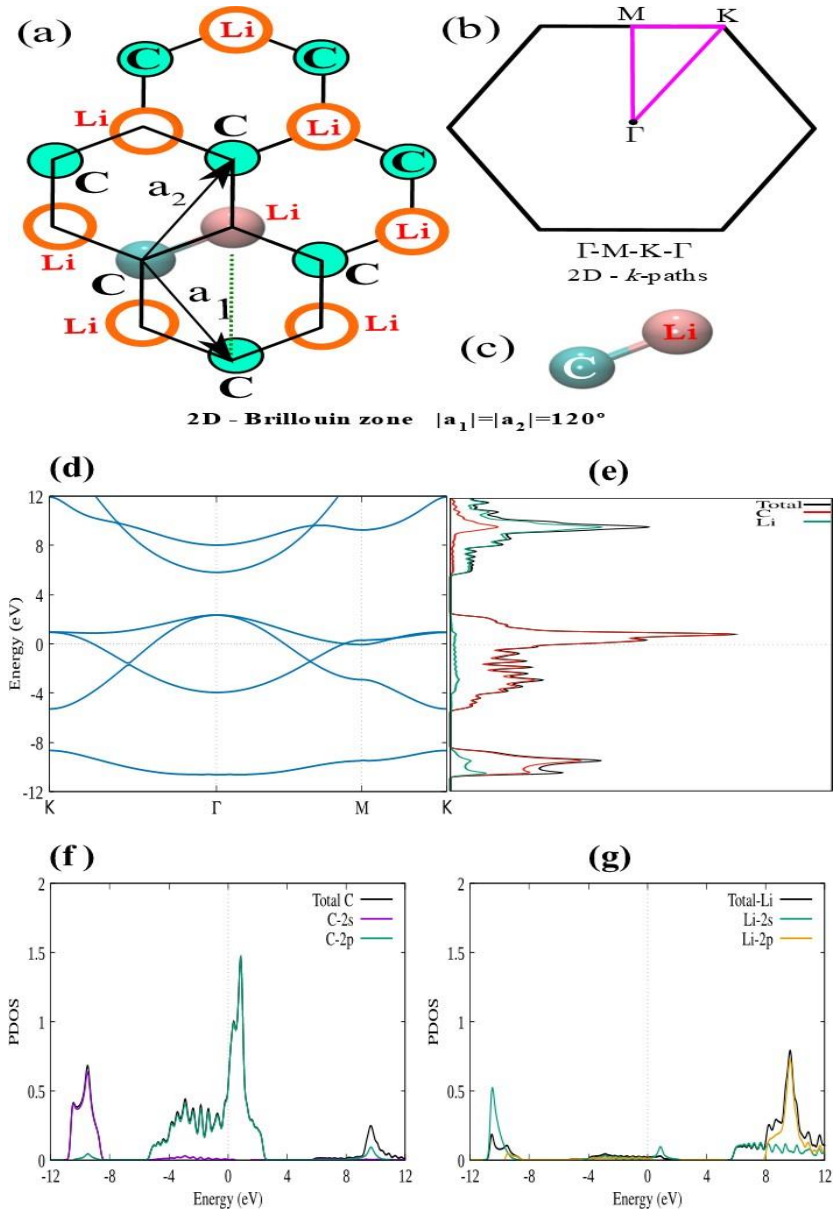


**Figure 5**: The electronic band structures of graphene single-layer doped C-Li. (a) Schematic illustration showed the reciprocal lattice vectors and the corners of the first Brillouin zone. (b) 2D-k-paths representation. (c) CPK fully atomistic visualization of C-Li bonded. (d) Electronic band structure and (e) density ofstates (DOS) and partial DOS (PDOS) of graphene single layer doping by Li atom. PDOS of (f) C atom and (g) Li atom in graphene single-layer doped C—Li.

Therefore, the electronic structure modification of graphene doped will be discussed in details in the following in this theoretical research work.

## 3. Results and discussion

graphene monolayer, where we replaced the element X, with chemical elements available in Pseudopotential GGAs Data base. Therefore, we obtein the relationship between energy band gap for all 55 combinations of doped graphene-based in chemical elements already showed.

In Figure 4 (d), the band structure of hydrogen atom-doped graphene is presented. Compared to pristine graphene, which is a semiconductor with a zero-band gap, the incorporation of hydrogen atoms induces a modification in the structure, resulting in a conductive state. Figures 4 (e), (f), and (g) depict the partial density of states corresponding to carbon and hydrogen atoms as well as their respective orbitals, revealing the significant contribution of hydrogen atoms to the formation of electronic density of states in the doped graphene structure.

Similarly, in Figure 5 (d), the band structure of lithium atom-doped graphene is portrayed. Unlike pristine graphene, the introduction of lithium atoms leads to the emergence of a band gap in the band structure. Furthermore, Figures 5 (e), (f), and (g) display the partial density of states corresponding to carbon and lithium atoms, including

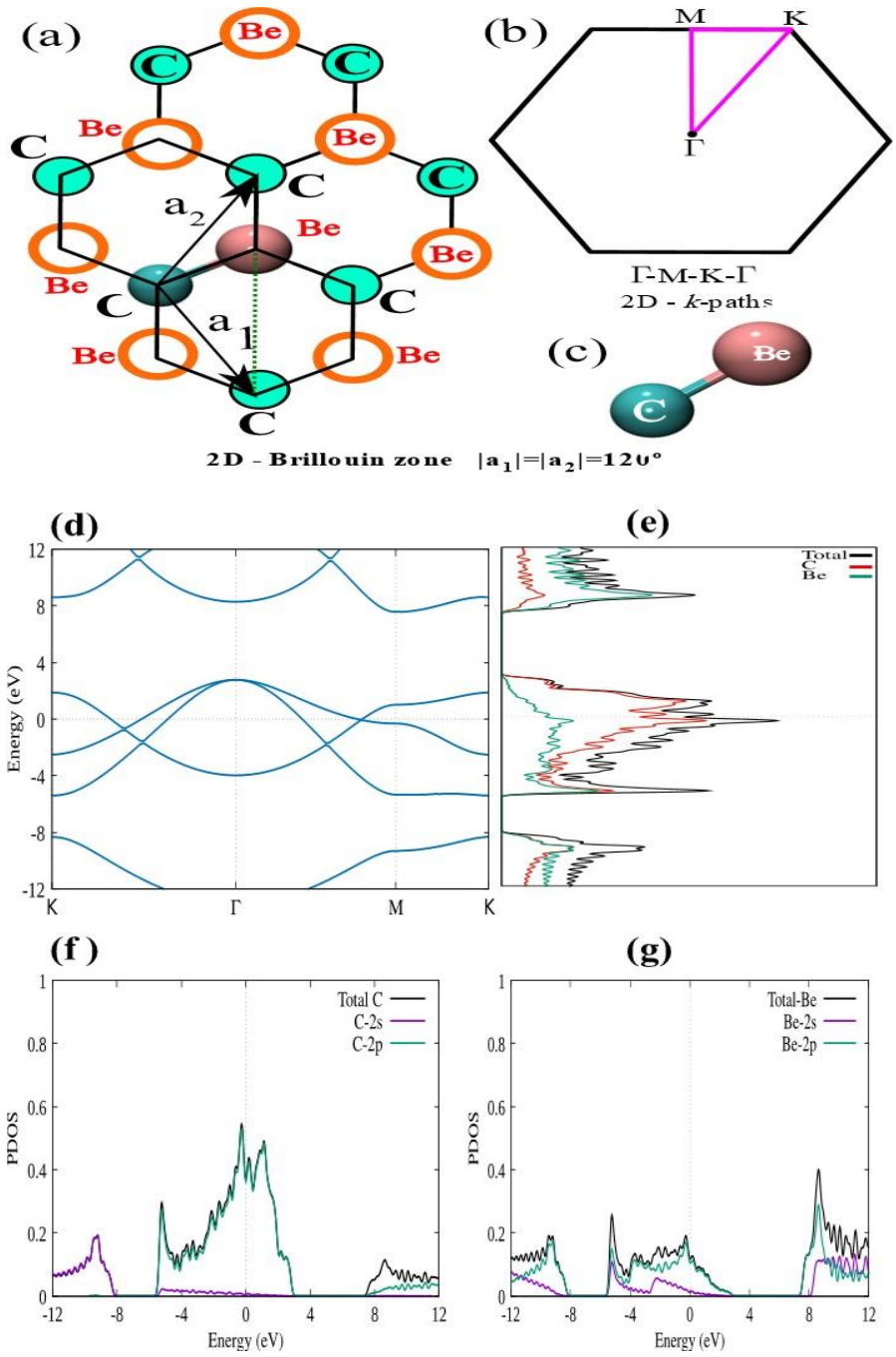


**Figure 6**: The electronic band structures of graphene single-layer doped C−Be. (a) Schematic illustrationshowed the reciprocal lattice vectors and the corners of the first Brillouin zone. (b) 2D-k-paths representation. (c) CPK fully atomistic visualization of C Be bonded. (d) Electronic band structure and (e) density of states (DOS) and partial DOS (PDOS) of graphene single layer doping by Be atom. PDOS of (f) C atom and (g) Be atom in graphene single-layer doped C−Be.

their respective orbitals, illustrating the impact of lithium atom doping on the electronic properties of graphene.

Figure 6 (d) presents the band structure of beryllium atom-doped graphene, showcasing a notable modification arising from the beryllium atom doping, which results in the emergence of new electronic states and altered band dispersion characteristics. This emphasizes the significant impact of beryllium atom doping on the electronic properties of graphene, introducing intriguing possibilities for tailored electronic applications.

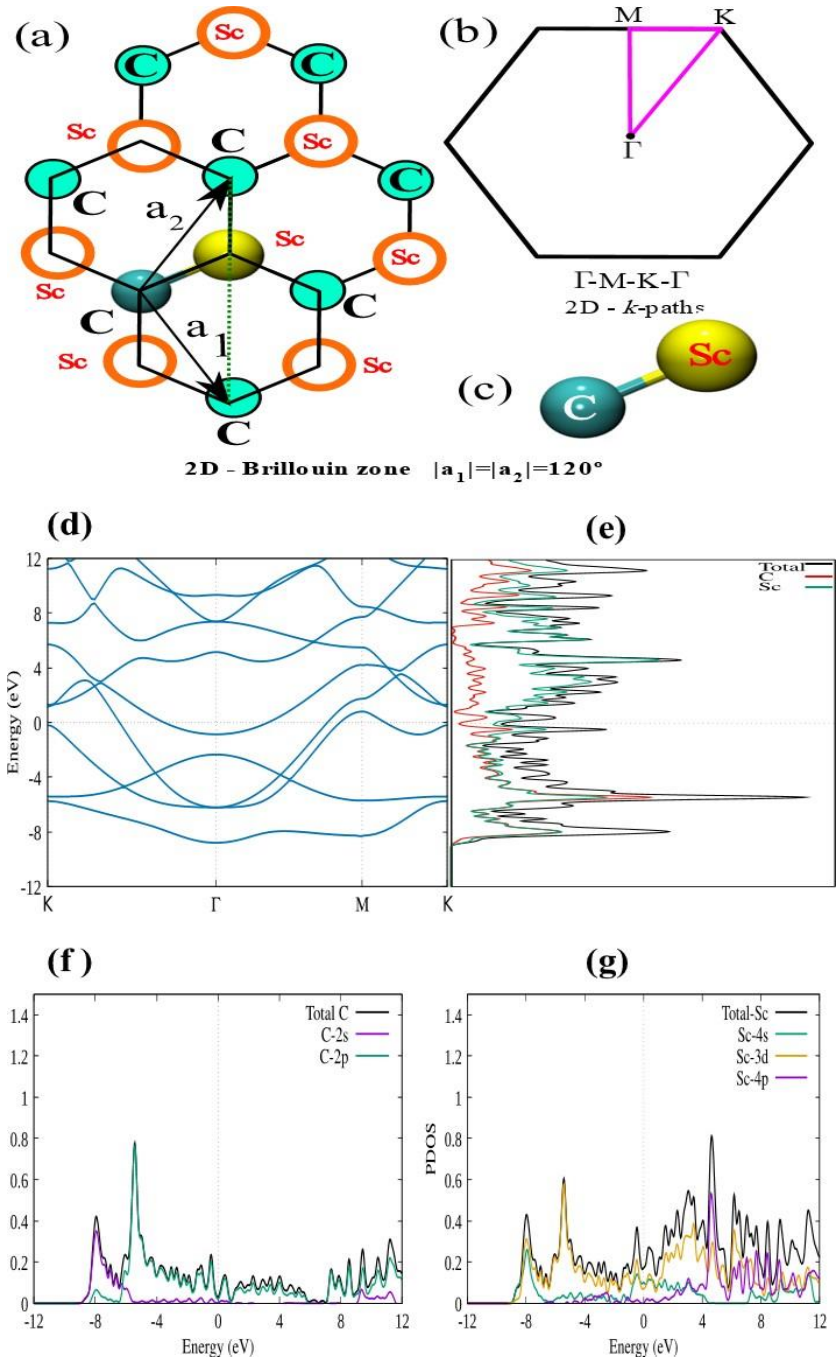


**Figure 7:** The electronic band structures of graphene single-layer doped C-Sc. (a) Schematic illustration showed the reciprocal lattice vectors and the corners of the first Brillouin zone. (b)2D-k-paths representation. (c) CPK fully atomistic visualization of C-Sc bonded. (d) Electronic band structure and (e) density of states (DOS) and partial DOS (PDOS) of graphene single layer doping by Sc atom. PDOS of (f) C atom and (g) Sc atom in graphene single-layer doped C-Sc.

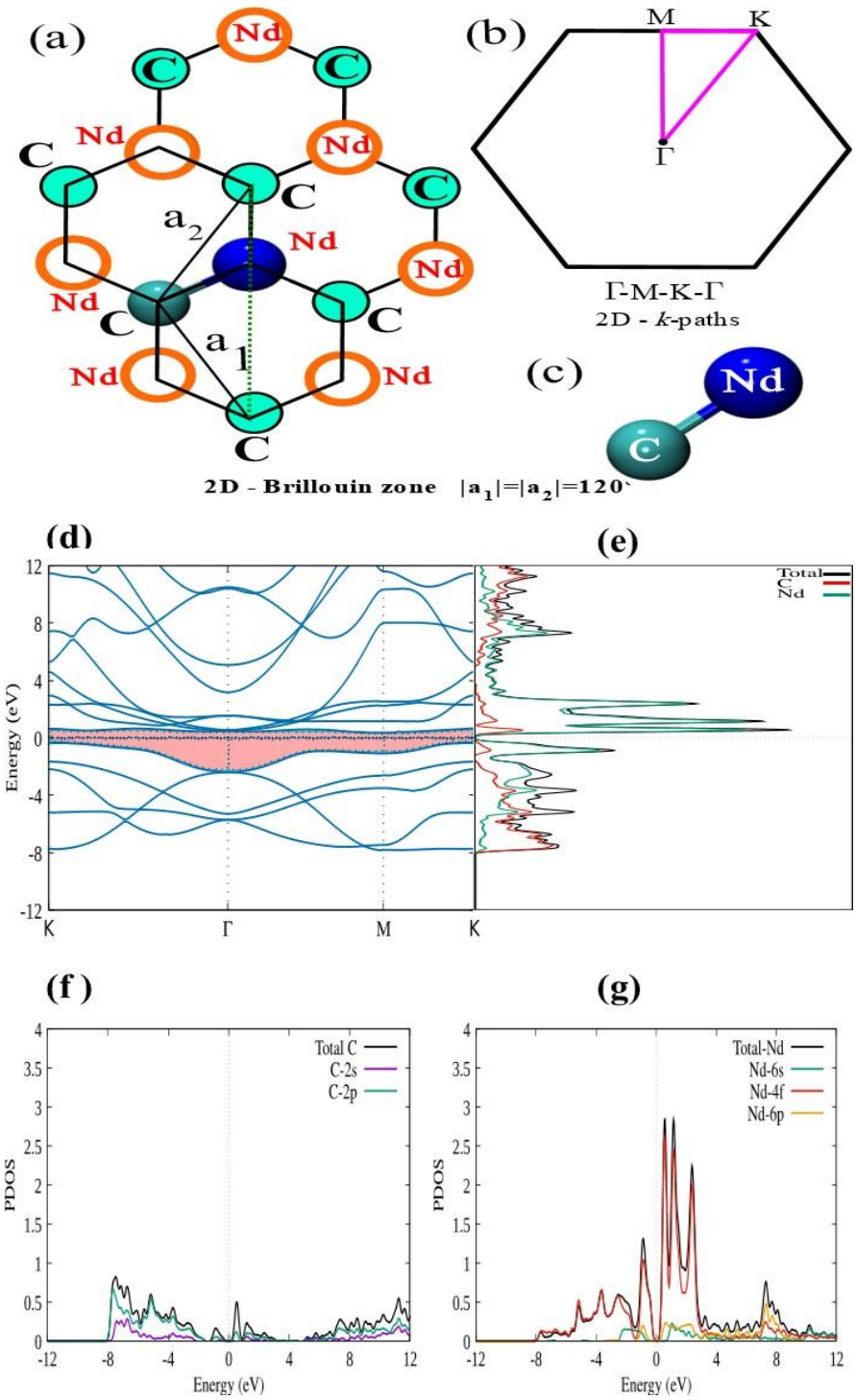


**Figure 8:** The electronic band structures of graphene single-layer doped C−Nd. (a) Schematic illustration showed the reciprocal lattice vectors and the corners of the first Brillouin zone. (b) 2D-k-paths representation. (c) CPK fully atomistic visualization of C Nd bonded. (d) Electronic band structure and (e) density of states (DOS) and partial DOS (PDOS) of graphene single layer doping by Nd atom. PDOS of (f) C atom and (g) Nd atom in graphene single-layer doped C−Nd.

In Figure 7 (d), illustrates the band structure of Scandium-doped graphene. to the band structure of graphene, which is a semiconductor with a zero-band gap, when we replace half of the carbon atoms of the graphene sheet with Sc atoms, the doped structure changes to a conductive state. Figure 7 (e), (f), and (g) shows the partial density of states corresponding to carbon and Scandium atoms and their orbitals respectively. According to Figure 7 (e), it can be observed that Scandium atoms have the highest contribution to the formation of electronic density of states. According to Figure 7 (f), it can be concluded that the contribution of 2*P* orbitals of the carbon atom is greater than its $2_s$ orbitals in the formation of the density of states. Also, according to Figure 7 (g), it can be seen that in the regions close to the Fermi level the $3_d$ orbitals of the Sc atom have a greater contribution than other orbitals in the formation of the density of

states. And after that, $4_s$ and $4_p$ orbitals have the largest contribution respectively.

gap of 0.773 eV is created in the doped structure. Figure 8 (e), (f), and (g) shows the partial density of states corresponding to carbon and

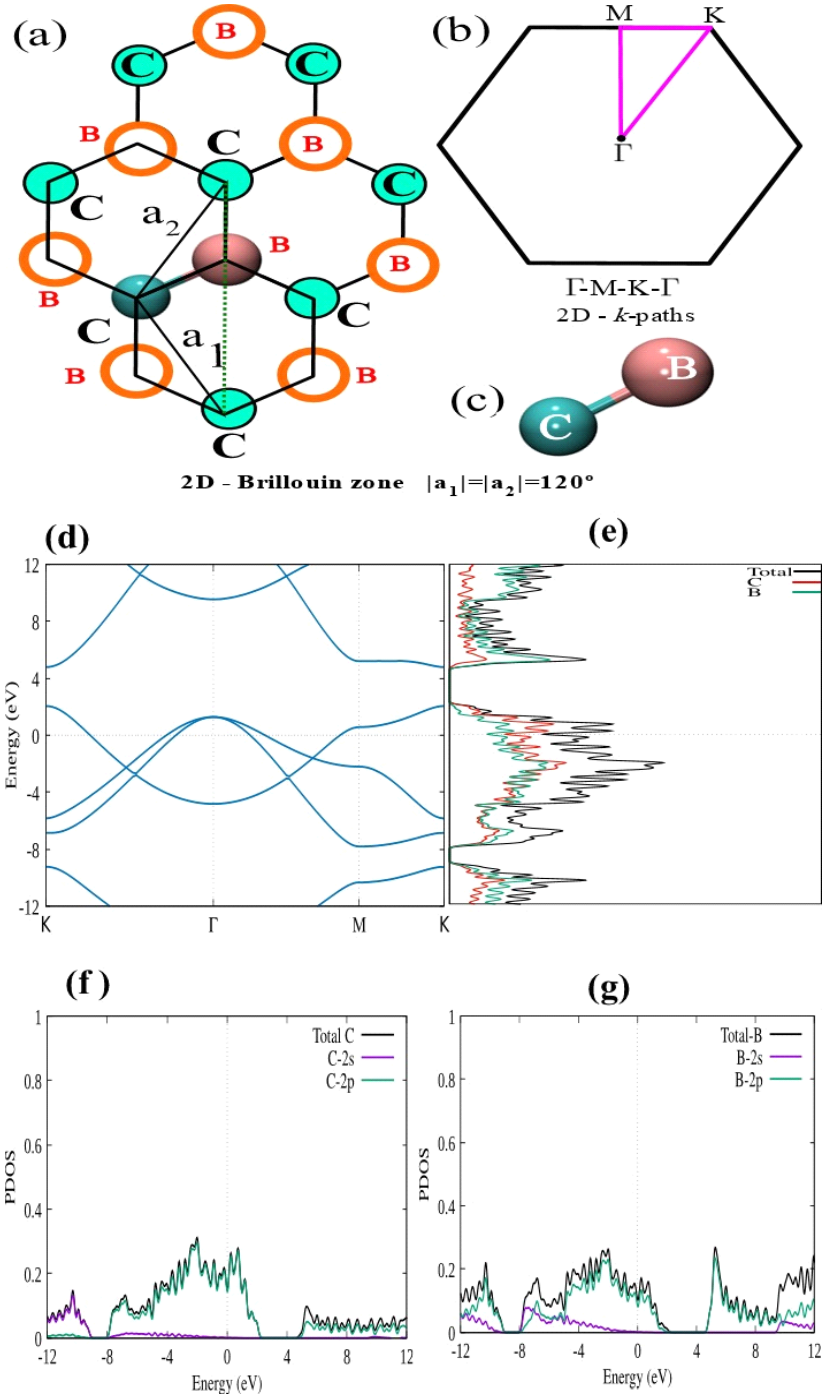


**Figure 9:** The electronic band structures of graphene single-layer doped C-B. (a) Schematic illustration showed the reciprocal lattice vectors and the corners of the first Brillouin zone. (b) 2D-k-paths representation. (c) CPK fully atomistic visualization of C B bonded. (d) Electronic band structure and (e) density of states(DOS) and partial DOS (PDOS) of graphene single layer doping by B atom. PDOS of (f) C atom and (g)B atom in graphene single-layer doped C−B.

In Figure 8 (d), illustrates the band structure of neodymium-doped graphene. According to which it can be seen that when half of the carbon atoms in the graphene sheet are replaced by Nd atoms (that is, 50% doping in the graphene structure is created using Nd atoms), a

neodymium atoms and their orbitals respectively. According to Figure 8 (e), it can be observed that neodymium atoms have the highest contribution to the formation of electronic density of states near the Fermi level and in the regions far from the Fermi level, the

contribution of carbon atoms dominates in the formation of the density of states. According to Figure 8 (f), it can be concluded that the contribution of $2_p$ orbitals of the carbon atom is greater than its $2_s$ orbitals in the formation of the density of states. Also, according to Figure 8 (g), which shows the partial density of states of the Nd atom, it can be seen that the $4_f$ orbitals of the Nd atom have a greater contribution than other orbitals in the formation of the density of states. And after that, $6_p$ and $6_s$ orbitals have the largest contribution respectively. Our computational results align well with experimental reports on doped graphene films, where the incorporation of dopant atoms modifies the π and π* bands and reduces the overall band gap [41]. Such consistency supports the reliability of the present simulation results in describing realistic doping-induced electronic modulation.

In Figure 9 p-type doping, trivalent impurities (elements with 3 valence electrons) are introduced into a semiconductor. One of the most common trivalent impurities is the boron atom (B). Here, we substitute half of the carbon atoms in the graphene structure with B atoms (50% doping with B atoms), resulting in p-type doping. Figure 9 (d), illustrates the band structure of boron-doped graphene. In comparison to the band structure of pristine graphene, due to the electron deficiency of boron, the Fermi level significantly shifts about 2.17 eV below the Dirac point and for this reason, the boron-doped graphene structure becomes a metal structure, unlike graphene, which is a semiconductor. Another important result is the creation of an energy gap of approximately 2.74 eV in the vicinity of the Dirac point. To determine the contributions of boron and carbon atoms, as well as their orbital contributions, to the formation of electronic density of states, the partial density of states corresponding to carbon and boron atoms and their orbitals are shown in Figures 9 (e), (f), and (g) respectively. According to Figure 9 (e), it can be observed that carbon atoms have the highest contribution to the formation of electronic density of states near the Fermi level. In the formation of density of states related to conduction bands, boron atoms have a higher contribution compared to carbon atoms. By examining Figures 9 (f), and (g), it can be concluded that for both carbon and boron atoms, their $2_P$ orbitals have a higher contribution compared to the $2_S$ orbitals in the formation of electronic density of states. It is worth noting that despite the promising electronic and optical tunability of doped graphene, scalable fabrication remains challenging. Achieving uniform dopant distribution, controlling defect density, and preserving the intrinsic lattice structure during large-area synthesis are key obstacles. Recent advances in chemical vapor deposition (CVD) growth and precursor optimization have demonstrated potential pathways to overcome these issues, paving the way toward reliable and scalable production of doped graphene materials [42].

It is important to note that the feasibility of dopant incorporation also depends on thermodynamic stability and kinetic barriers. These aspects were not considered in the present work, which focuses primarily on the electronic structure of substitutionally doped graphene/PGNTs. The results presented here are therefore limited to the electronic band structures and PDOS analyses, without explicit optical-property calculations. Nevertheless, the computed electronic characteristics provide valuable insights for potential device applications. (i) Dopants that open moderate band gaps (on the order of a few tenths of an eV) may serve as promising candidates for semiconductor channels in nanoscale transistors, provided carrier mobility is preserved. (ii) Dopants that induce substantial Fermi-level shifts (n-type or p-type behavior) can be utilized for contact engineering or work-function tuning in electrode materials. (iii) Dopants that create sharp, localized mid-gap states could find use in chemical or gas sensors, where these states are sensitive to adsorbates, or as localized trap/spin centers for quantum applications. These application-oriented implications are based solely on the electronic-structure trends obtained in this study. Future investigations should include formation energy analysis and *ab initio* molecular dynamics to assess thermodynamic and kinetic dopability, as well as optical-property and charge-transport calculations (e.g., GW-BSE or time-dependent DFT approaches) to comprehensively evaluate the suitability of these doped systems for real-world nanoelectronic and optoelectronic applications

## 4. Conclusions and remarks

In this study, we used density functional theory to examine how doping graphene with different elements changes its electronic properties. Our results show that doping can make graphene either more conductive or behave like a semiconductor, depending on the element used. For example, hydrogen and scandium doping improve graphene's conductivity by adding states that help electrons move more easily. Lithium and beryllium cause graphene to develop an energy gap, turning it into a semiconductor material. Neodymium doping also creates a moderate energy gap of about 0.77 eV, which is useful for electronic devices. Boron doping has an even larger effect, opening a strong energy gap of about 2.74 eV and shifting energy levels so graphene acts like a metal with p-type behavior. This means we can carefully choose which elements to add to graphene to control its electrical behavior. Such control is very important for designing new graphene-based electronic devices that need specific properties, like fast electronics or sensors. Overall, our study shows that element-

specific doping is a powerful way to tune graphene's electronic features for various applications.

**Authors' contributions:** Not applicable.

**Declaration of competing interest**: Not applicable.

**Funding:** This paper received no external funding.

**Data availability:** Not applicable.

**References**

[1] Novoselov, K.S., Geim, A.K., Morozov, S.V., Jiang, D.-E., Zhang, Y., Dubonos, S.V., Grigorieva, I.V. Electric field effect in atomically thin carbon films. *Science*. **2004**, 306(5696), 666–669.

[2] Neto, A.C., Guinea, F., Peres, N.M., Novoselov, K.S., Geim, A.K. The electronic properties of graphene. *Reviews of Modern Physics*. **2009**, 81(1), 109.

[3] Novoselov, K.S., Geim, A.K., Morozov, S.V., Jiang, D., Katsnelson, M.I., Grigorieva, I.V. Two-dimensional gas of massless Dirac fermions in graphene. *Nature*. **2005**, 438(7065), 197–200.

[4] Nair, R.R., Blake, P., Grigorenko, A.N., Novoselov, K.S., Booth, T.J., Stauber, T., Peres, N.M., Geim, A.K. Fine structure constant defines visual transparency of graphene. *Science*. **2008**, 320(5881), 1308.

[5] Katsnelson, M.I., Novoselov, K.S., Geim, A.K. Chiral tunnelling and the Klein paradox in graphene. *Nature Physics*. **2006**, 2(9), 620–625.

[6] Wu, H., Drzal, L.T. Graphene nanoplatelet paper as a light-weight composite with excellent electrical and thermal conductivity and good gas barrier properties. *Carbon*. **2012**, 50(3), 1135–1145.

[7] Lin, Y.-M., Dimitrakopoulos, C., Jenkins, K.A., Farmer, D.B., Chiu, H.-Y., Grill, A., Avouris, P. 100-GHz transistors from wafer-scale epitaxial graphene. *Science*. **2010**, 327(5966), 662.

[8] Mayorov, A., Elias, D., Mucha-Kruczynski, M., Gorbachev, R., Tudorovskiy, T., Zhukov, A., Morozov, S., Katsnelson, M., Fal'ko, V., Geim, A.K., et al. Interaction-driven spectrum reconstruction in bilayer graphene. *Science*. **2011**, 333(6044), 860–863.

[9] Yang, X., Liu, G., Rostami, M., Balandin, A.A., Mohanram, K. Graphene ambipolar multiplier phase detector. *IEEE Electron Device Letters*. **2011**, 32(10), 1328–1330.

[10] Lee, C., Wei, X., Kysar, J.W., Hone, J. Measurement of the elastic properties and intrinsic strength of monolayer graphene. *Science*. **2008**, 321(5887), 385–388.

[11] Lee, J.-U., Yoon, D., Cheong, H. Estimation of Young's modulus of graphene by Raman spectroscopy. *Nano Letters*. **2012**, 12(9), 4444–4448.

[12] Jiang, J.-W., Wang, J.-S., Li, B. Young's modulus of graphene: a molecular dynamics study. *Physical Review B*. **2009**, 80(11), 113405.

[13] de Sousa, J.M. Nanostructures failures and fully atomistic molecular dynamics simulations. In: *Elasticity of Materials*. IntechOpen, **2021**.

[14] Balandin, A.A., Ghosh, S., Bao, W., Calizo, I., Teweldebrhan, D., Miao, F., Lau, C.N. Superior thermal conductivity of single-layer graphene. *Nano Letters*. **2008**, 8(3), 902–907.

[15] Wang, X., Zhi, L., Müllen, K. Transparent, conductive graphene electrodes for dye-sensitized solar cells. *Nano Letters*. **2008**, 8(1), 323–327.

[16] Craciun, M.F., Russo, S., Yamamoto, M., Tarucha, S. Tuneable electronic properties in graphene. *Nano Today*. **2011**, 6(1), 42–60.

[17] Zhan, D., Yan, J., Lai, L., Ni, Z., Liu, L., Shen, Z. Engineering the electronic structure of graphene. *Advanced Materials*. **2012**, 24(30), 4055–4069.

[18] Wang, X., Sun, G., Routh, P., Kim, D.-H., Huang, W., Chen, P. Heteroatom-doped graphene materials: syntheses, properties and applications. *Chemical Society Reviews*. **2014**, 43(20), 7067–7098.

[19] Putri, L.K., Ong, W.-J., Chang, W.S., Chai, S.-P. Heteroatom-doped graphene in photocatalysis: a review. *Applied Surface Science*. **2015**, 358, 2–14.

[20] Shao, Y., Zhang, S., Engelhard, M.H., Li, G., Shao, G., Wang, Y., Liu, J., Aksay, I.A., Lin, Y. Nitrogen-doped graphene and its electrochemical applications. *Journal of Materials Chemistry*. **2010**, 20(35), 7491–7496.

[21] Kumar, R., Sahoo, S., Joanni, E., Singh, R.K., Maegawa, K., Tan, W.K., Kawamura, G., Kar, K.K., Matsuda, A. Heteroatom-doped graphene engineering for energy storage and conversion. *Materials Today*. **2020**, 39, 47–65.

[22] Vargas-Bernal, R. Graphene against other two-dimensional materials: a comparative study on the basis of electronic properties. In: *Two-Dimensional Materials: Synthesis, Characterization and Potential Applications*. **2016**, 103.

[23] Wang, Y., et al. Theoretical studies on the structures and properties of doped graphenes with and without an external electrical field. *RSC Advances*. **2019**, 9(21), 11939–11950.

[24] Hohenberg, P., Kohn, W. Inhomogeneous electron gas. *Physical Review*. **1964**, 136(3B), B864.

[25] Kohn, W., Sham, L.J. Self-consistent equations including exchange and correlation effects. *Physical Review*. **1965**, 140(4A), A1133.

[26] Soler, J.M., Artacho, E., Gale, J.D., García, A., Junquera, J., Ordejón, P., Sánchez-Portal, D. The SIESTA method for ab initio order-N materials simulation. *Journal of Physics: Condensed Matter*. **2002**, 14(11), 2745–2779.

[27] Artacho, E., Anglada, E., Diéguez, O., Gale, J.D., García, A., Junquera, J., Martin, R.M., Ordejón, P., Pruneda, J.M., Sánchez-Portal, D., et al. The SIESTA method: developments and applicability. *Journal of Physics: Condensed Matter*. **2008**, 20(6), 064208.

[28] Artacho, E., Sánchez-Portal, D., Ordejón, P., Garcia, A., Soler, J.M. Linear-scaling ab initio calculations for large and complex systems. *Physica Status Solidi (b)*. **1999**, 215(1), 809–817.

[29] Pinto, A.M., et al. Smaller particle size and higher oxidation improves biocompatibility of graphene-based materials. *Carbon*. **2016**, 99, 318–329.

[30] Anglada, E., Soler, J.M., Junquera, J., Artacho, E. Systematic generation of finite-range atomic basis sets for linear-scaling calculations. *Physical Review B*. **2002**, 66(20), 205101.

[31] Perdew, J.P., Burke, K., Ernzerhof, M. Generalized gradient approximation made simple. *Physical Review Letters*. **1996**, 77(18), 3865.

[32] Troullier, N., Martins, J.L. Efficient pseudopotentials for plane-wave calculations. *Physical Review B*. **1991**, 43(3), 1993.

[33] Kleinman, L., Bylander, D. Efficacious form for model pseudopotentials. *Physical Review Letters*. **1982**, 48(20), 1425.

[34] Monkhorst, H.J., Pack, J.D. Special points for Brillouin-zone integrations. *Physical Review B*. **1976**, 13(12), 5188.

[35] Wallace, P.R. The band theory of graphite. *Physical Review*. **1947**, 71(9), 622

[36] Saito, R., Fujita, M., Dresselhaus, G., Dresselhaus, M.S. Electronic structure of graphene tubules based on C60. *Physical Review B*. **1992**, 46(3), 1804.

[37] Akhiezer, A.I. *Quantum Electrodynamics*. **1965**.

[38] Schedin, F., Geim, A.K., Morozov, S.V., Hill, E.W., Blake, P., Katsnelson, M.I., Novoselov, K.S. Detection of individual gas molecules adsorbed on graphene. *Nature Materials*. **2007**, 6(9), 652–655.

[39] Das, A., Pisana, S., Chakraborty, B., Piscanec, S., Saha, S.K., Waghmare, U.V., Novoselov, K.S., Krishnamurthy, H.R., Geim, A.K., Ferrari, A.C., et al. Monitoring dopants by Raman scattering in an electrochemically top-gated graphene transistor. *Nature Nanotechnology*. **2008**, 3(4), 210–215.

[40] Miller, D.L., Kubista, K.D., Rutter, G.M., Ruan, M., de Heer, W.A., First, P.N., Stroscio, J.A. Observing the quantization of zero-mass carriers in graphene. *Science*. **2009**, 324(5929), 924–927.

[41] Joucken, F., Frédéric, L., Luc, H., Jérôme, L. Electronic properties of chemically doped graphene. *Physical Review Materials*. **2019**, 3(11), 110301.

[42] Chen, K., et al. Scalable chemical-vapour-deposition growth of three-dimensional graphene materials towards energy-related applications. *Chemical Society Reviews*. **2018**, 47(9), 3018–3036